Solar Energy
And Sustainable Development
Refereed, biannual scientific journal issued by:
The Libyan Center for Solar Energy Research and Studies

Phosphorus Doping Effects on the Optoelectronic Properties of $K_2AgAsBr_6$ Double Perovskites for Photovoltaic Applications

Abdelmounaim Laassouli[1]*, Lhouceine Moulaoui[2], Abdelhafid Najim[3], Hamza Errahoui[4]. Khalid Rahmani[5], Youssef Lachtioui[6], Omar Bajjou[7].

[1,3,4,6,7]Laboratory of Engineering in Chemistry and Physics of Matter (LICPM), Faculty of Sciences and Technics, Sultan Moulay Slimane University, BP 523, 23000 Beni Mellal, Morocco
[2]Research Laboratory in Physics and Sciences for Engineers (LRPSI), Poly-disciplinary Faculty, Sultan Moulay Slimane University, BP 592, 23000 Beni Mellal, Morocco
[7]UNESCO UNISA Africa Chair in Nanosciences & Nanotechnology (U2ACN2), College of Graduate Studies, University of South Africa (UNISA), Pretoria, South Africa
[5]PSES, ERC, Ecole Normale Supérieure, Mohammed V University in Rabat P. O. Box: BP5118 Takkadoum Rabat-10000, Morocco.

E-*mail:* [1] abdelmounaim.laassouli@gmail.com .

SPECIAL ISSUE ON:

The 2024 1st International Conference on Materials Sciences and Mechatronics for Sustainable Energy and the Environment
October 1-3, 2024 at Béni-Mellal, Morocco

KEYWORDS

double perovskites, phosphorus doping, photoelectric devices, DFT calculations, band gap.

ABSTRACT

This work explores the modifications of optoelectronic properties in $K_2AgAsBr_6$ double perovskites induced by phosphorus doping. First-principles calculations using the CASTEP code with the PBE functional were carried out based on density functional theory (DFT). Our research investigates the electronic structure and optical behavior of the cubic Fm-3m phase of $K_2AgAsBr_6$, $K_2AgAs_{0.8}P_{0.2}Br_6$, and $K_2AgAs_{0.6}P_{0.4}Br_6$ to elucidate the impact of progressive phosphorus (P) substitution.

P was chosen for its potential to modify the electronic structure due to its smaller atomic radius and different valence orbital energies compared to As. Our results reveal a systematic narrowing of the band gap with increasing P content, from 0.749 eV for the undoped compound to 0.587 eV for $K_2AgAs_{0.8}P_{0.2}Br_6$ and 0.424 eV for $K_2AgAs_{0.6}P_{0.4}Br_6$. This trend is attributed to the upward shift of the valence band maximum due to the higher energy of P 3p orbitals compared to As 4p orbitals. Analysis of the density of states confirms increased hybridization between P-p and As-p states at the valence band edge. Optical properties, including absorption coefficient, dielectric function, refractive index, and extinction coefficient, demonstrate a consistent red-shift and broadening of spectral features with P doping. Notably, P-substituted compounds exhibit enhanced absorption in the visible light region, with up to a 20% increase in the absorption coefficient at 550 nm for $K_2AgAs_{0.6}P_{0.4}Br_6$ compared to the undoped compound.

*Corresponding author.

DOI: https://doi.org/10.51646/jsesd.v14iSI_MSMS2E.407

This study reveals that elemental substitution offers a viable route to tailor optical and electronic properties of double perovskites, paving the way for the design of novel materials for next-generation photovoltaic and photoelectric devices.

تأثيرات تطعيم الفوسفور على الخواص البصرية والإلكترونية لمركبات بيروفسكايت المزدوجة $K_2AgAsBr_6$ لتطبيقات الطاقة الشمسية

عبد المنعم العسولي، الحسين مولاوي، عبد الحفيظ نجيم، حمزة الرحوي، خالد الرحماني، يوسف الشتيوي، عمر باجو.

ملخص: يتناول هذا العمل دراسة التعديلات في الخصائص البصرية والإلكترونية لمركبات البيروفسكايت المزدوجة $K_2AgAsBr_6$ الناتجة عن تطعيمها بالفوسفور. تم إجراء حسابات من المبادئ الأولى باستخدام شفرة CASTEP مع دالة PBE، بناءً على نظرية الكثافة الوظيفية (DFT).

يركز بحثنا على دراسة البنية الإلكترونية والسلوك البصري للطور المكعب Fm-3m للمركبات $K_2AgAsBr_6$، و $K_2AgAs_{0.8}P_{0.2}Br_6$، و $K_2AgAs_{0.6}P_{0.4}Br_6$ لفهم تأثير الاستبدال التدريجي بالفوسفور (P). تم اختيار الفوسفور نظرًا لقدرته على تعديل البنية الإلكترونية بفضل نصف قطره الذري الأصغر وطاقة مدارات تكافؤه المختلفة مقارنة بالزرنيخ (As). أظهرت نتائجنا انخفاضًا منهجيًا في فجوة الطاقة مع زيادة محتوى الفوسفور، حيث انخفضت فجوة الطاقة من 0.749 إلكترون فولت للمركب غير المطعم إلى 0.587 إلكترون فولت لـ $K_2AgAs_{0.8}P_{0.2}Br_6$ و0.424 إلكترون فولت لـ $K_2AgAs_{0.6}P_{0.4}Br_6$. يُعزى هذا الاتجاه إلى ارتفاع مستوى أعلى شريط تكافؤ نتيجة للطاقة الأعلى لمدارات P-3p مقارنة بمدارات As-4p. أكدت تحليلات كثافة الحالات حدوث زيادة في التهجين بين حالات P-p وAs-p عند حافة شريط التكافؤ. أما الخصائص البصرية، بما في ذلك معامل الامتصاص، والدالة العازلة، ومعامل الانكسار، ومعامل الانقراض، فقد أظهرت انزياحًا طيفيًا نحو الأحمر وزيادة في اتساع الميزات الطيفية مع تطعيم الفوسفور. ومن الجدير بالذكر أن المركبات المطعمة بالفوسفور أظهرت تحسينًا في الامتصاص في منطقة الضوء المرئي، مع زيادة تصل إلى 20% في معامل الامتصاص عند الطول الموجي 550 نانومتر للمركب $K_2AgAs_{0.6}P_{0.4}Br_6$ مقارنة بالمركب غير المطعم. تُظهر هذه الدراسة أن الاستبدال العنصري يقدم مسارًا فعالًا لتعديل الخصائص البصرية والإلكترونية لمركبات البيروفسكايت المزدوجة، مما يمهد الطريق لتصميم مواد جديدة لأجهزة الفوتوفولتيك والتطبيقات الكهروضوئية من الجيل القادم..

الكلمات المفتاحية – البيروفسكايت المزدوج، التطعيم بالفوسفور، الأجهزة الكهروضوئية، حسابات DFT، فجوة الطاقة.

1. INTRODUCTION

Halide perovskites have gained significant attention due to their outstanding optoelectronic characteristics and potential use in solar cells and other electronic devices [1]. Among these, double perovskites have emerged as an intriguing class of materials, offering enhanced stability and tunable properties. $K_2AgAsBr_6$ [2], a lead-free double perovskite, has shown promise as a stable compound with an indirect band gap. However, its wide band gap limits its effectiveness in absorbing sunlight, hindering its application in solar energy conversion [3]. In this study, we employ first-principles calculations grounded in DFT to address several key objectives aimed at enhancing the material's performance. Our primary goals are to investigate phosphorus doping as a strategic approach for band gap engineering in $K_2AgAsBr_6$, leveraging P's smaller atomic radius and different valence orbital energies compared to arsenic [4]; to elucidate the fundamental mechanisms by which P substitution influences the electronic structure and band properties of the host material; to quantitatively assess the enhancement in optical properties and solar absorption capabilities through systematic characterization of P-doped variants; and to establish design principles for the development of improved perovskite-based photovoltaic materials[5]. Through comprehensive investigation of $K_2AgAsBr_6$ and its phosphorus-doped variants ($K_2AgAs_{0.8}P_{0.2}Br_6$ and $K_2AgAs_{0.6}P_{0.4}Br_6$), we examine key parameters including band structure, density of states, absorption coefficient, dielectric function, refractive index, and

extinction coefficient to understand how progressive P substitution affects these properties [6]. The inherent tunability of perovskites through elemental substitution makes this investigation particularly relevant for advancing our understanding of band gap engineering strategies [7]. This study employs first-principles calculations grounded in DFT to explore the electronic and optical characteristics of $K_2AgAsBr_6$ and its phosphorus-doped variants, $K_2AgAs_{0.8}P_{0.2}Br_6$ and $K_2AgAs_{0.6}P_{0.4}Br_6$. Through examining aspects such as band structure, density of states, absorption coefficient, dielectric function, refractive index, and extinction coefficient, this study seeks to comprehensively investigate the influence of phosphorus doping on the optoelectronic characteristics of $K_2AgAsBr_6$. this research investigates the impact of progressive P substitution on these properties, seeking to elucidate the potential of P doping for enhancing the performance of $K_2AgAsBr_6$ in optoelectronic applications [8], particularly for efficient solar energy conversion [9]. This research provides valuable insights for the development and refinement of advanced materials for use in next-generation photovoltaic and optoelectronic devices, potentially paving the way for more efficient and stable lead-free perovskite materials.

2. METHOD OF CALCULATIONS

The electronic and optical properties of $K_2AgAsBr_6$ perovskite were modeled using density functional theory (DFT) calculations using the CASTEP code [10], The PBE exchange-correlation functional was used in our calculations since it serves within the generalized gradient approximation (GGA) framework for determining the exchange-correlation energy of the system [11]. Representations of the contributions of core and valence electrons were performed with ultrasoft pseudopotentials. Electron-ion interactions were described using on-the-fly generated (OTFG) pseudopotentials as described in [12].

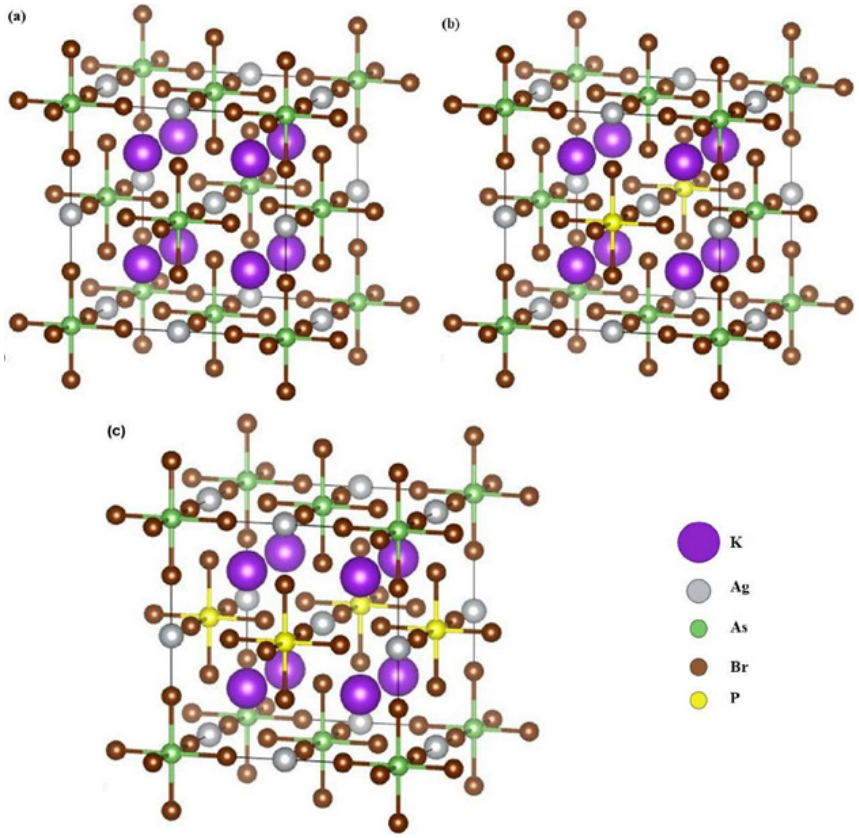

Figure 1. Crystal structure of $K_2AgAsBr_6$ (a), $K_2AgAs_{0.8}P_{0.2}Br_6$(b), and $K_2AgAs_{0.6}P_{0.4}Br_6$ (c)

The calculations were carried out with a plane wave basis set with an energy cutoff of 500 eV. The

primary unit cell was sampled with a 2 × 2 × 2 k-point grid, providing sufficient convergence for the analysis of the electronic structure. In the self-consistent field operations, the Pulay density mixing method was used, and the convergence criterion was set at 2×10^{-5} eV/atom [13]. The maximum stress was defined to be 0.1 GPa [14]. Valence electron configurations were as follows: K: $3s^2 3p^6 4s^1$, Ag: $4d^{10} 5s^1$, As: $4s^2 4p^3$, Br: $4s^2 4p^5$, and P: $3s^2 3p^3$. The geometry of the $K_2AgAsBr_6$ structure was optimized before calculating electronic and optical properties. A supercell of cubic $K_2AgAsBr_6$ structure with Fm3m symmetry with lattice parameters a = b = c = 10.95 Å and α = β = γ = 90° was studied. Different P doping concentrations were investigated by systematically replacing specific As atoms with P atoms in the supercell (see Figure 1).

3. RESULTS AND DISCUSSION

3.1. Electronic Properties

3.1.1. Band Gap

The calculated electronic band structures of $K_2AgAsBr_6$, $K_2AgAs_{0.8}P_{0.2}Br_6$, and $K_2AgAs_{0.6}P_{0.4}Br_6$ (Figure 2) reveal a clear trend in electronic properties with increasing phosphorus content. All three compounds exhibit semiconducting behavior with indirect band gaps located at the high-symmetry point. Notably, a systematic narrowing of the band gap is observed as phosphorus substitution increases. The band gap of the undoped $K_2AgAsBr_6$ is calculated to be 0.749 eV [15], decreasing to 0.584 eV and 0.424 eV for $K_2AgAs_{0.8}P_{0.2}Br_6$ and $K_2AgAs_{0.6}P_{0.4}Br_6$, respectively. This reduction in band gap is attributed to the higher energy of P 3p orbitals compared to As 4p orbitals, leading to an upward shift of the valence band maximum. The reduced band gap (0.424 eV for $K_2AgAs_{0.6}P_{0.4}Br_6$) and enhanced visible light absorption make these materials particularly suitable for single-junction and tandem solar cells. Despite the band gap narrowing, the overall features of the band structure, including the dispersion of conduction and valence bands, remain qualitatively similar across the three compositions.

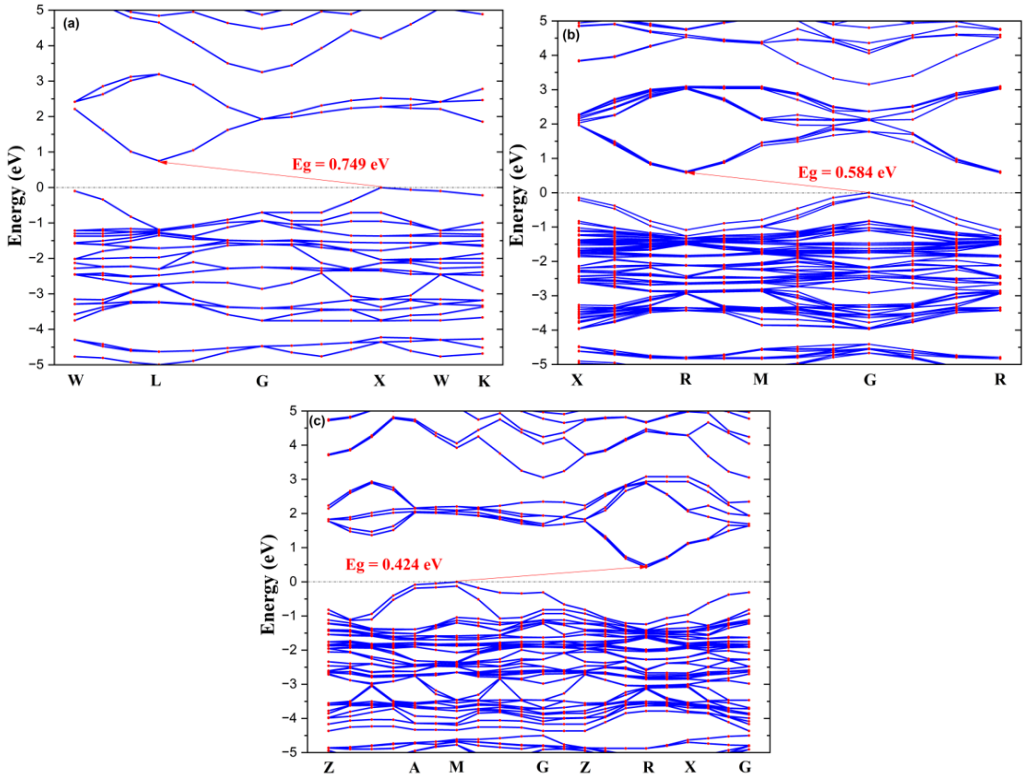

Figure 2. Band structures of $K_2AgAsBr_6$ (a), $K_2AgAs_{0.8}P_{0.2}Br_6$(b), and $K_2AgAs_{0.6}P_{0.4}Br_6$ (c).

3.1.2. Density of States

The Total Density of States (TDOS) for $K_2AgAsBr_6$, $K_2AgAs_{0.8}P_{0.2}Br_6$, and $K_2AgAs_{0.6}P_{0.4}Br_6$ is shown in (Figure 3), highlighting the electronic structure variations resulting from phosphorus doping. These TDOS graphs exhibit a uniform trend across the three compositions, with the Fermi level (Ef) positioned at 0 eV [16]. As the phosphorus content increases, we observe a notable increase in the density of states near the Fermi level, particularly in the valence band region. This trend is evident from the heightened peaks and increased complexity of features in the TDOS plots of the phosphorus-doped compounds compared to the undoped $K_2AgAsBr_6$. The enhanced DOS near the Fermi level for $K_2AgAs_{0.8}P_{0.2}Br_6$ and $K_2AgAs_{0.6}P_{0.4}Br_6$ suggests an increase in the number of available electronic states, which could contribute to improved charge carrier transport properties. Furthermore, the gradual reduction of the band gap, as indicated by the narrowing of the zero-state region around the Fermi level, corroborates the band structure analysis.

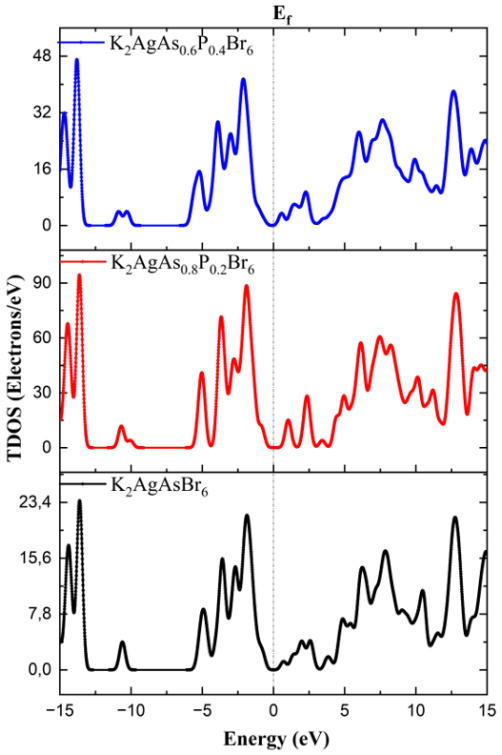

Figure 3. TDOS of $K_2AgAsBr_6$, $K_2AgAs_{0.8}P_{0.2}Br_6$, and $K_2AgAs_{0.6}P_{0.4}Br_6$.

The Partial Density of States (PDOS) calculations, presented in (Figure 4), elucidate the orbital-specific contributions to the electronic structure. Analysis reveals that the valence band maximum is primarily composed of Br-p and As-p states, with minor contributions from Ag-d states. The conduction band minimum is dominated by Ag-s and Ag-p states. With increasing phosphorus content, P-p states emerge and intensify near Ef, particularly in the valence band region, indicating enhanced hybridization between P-p and As-p orbitals. This hybridization likely contributes to the observed band gap narrowing. The K states remain largely unchanged and contribute minimally near the Fermi level, suggesting their limited role in determining the compounds' electronic properties.

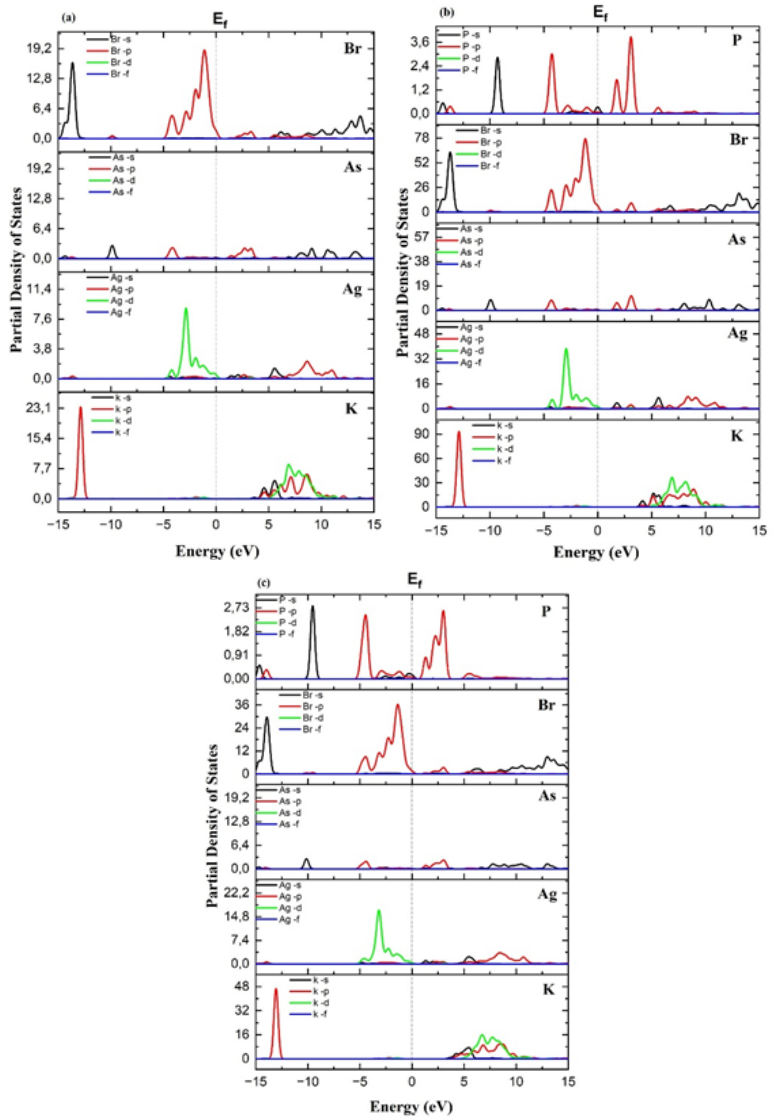

Figure 4. PDOS of $K_2AgAsBr_6$, $K_2AgAs_{0.8}P_{0.2}Br_6$, and $K_2AgAs_{0.6}P_{0.4}Br_6$.

3.2. Optical Properties

3.2.1. Absorption Coefficient

The absorption coefficient (α) quantifies the depth to which light can penetrate a material before being significantly absorbed [17]. This parameter is crucial for understanding and optimizing the efficiency of solar energy conversion systems. The absorption coefficient can be calculated using:

$$\alpha(\omega) = 2\omega\sqrt{\frac{-\varepsilon_1(\omega)}{2} + \sqrt{\frac{(\varepsilon_1(\omega))^2 + (\varepsilon_2(\omega))^2}{2}}} \qquad (1)$$

where $\varepsilon_1(\omega)$ and $\varepsilon_2(\omega)$ are the real and imaginary parts of the dielectric function, respectively [18]. Analysis of optical absorption spectra reveals a systematic bathochromic shift of the absorption edge with increasing phosphorus substitution in the $K_2AgAs_{1-x}P_xBr_6$ system. Optical absorption coefficients were determined for three compositions: the parent compound $K_2AgAsBr_6$ and two phosphorus-substituted derivatives, $K_2AgAs_{0.8}P_{0.2}Br_6$ and $K_2AgAs_{0.6}P_{0.4}Br_6$ (Figure 5). The spectroscopic data demonstrate that increasing phosphorus content directly correlates with enhanced visible-light absorption capabilities.The parent compound $K_2AgAsBr_6$ exhibits strong absorption predominantly in the ultraviolet region ($\lambda < 400$ nm), whereas the phosphorus-

substituted compounds display progressively red-shifted absorption edges extending into the visible spectrum. This systematic shift corresponds to the band gap narrowing observed in electronic structure calculations. The expanded spectral response of $K_2AgAs_{0.8}P_{0.2}Br_6$ and $K_2AgAs_{0.6}P_{0.4}Br_6$ in the visible region indicates that these materials are particularly promising for photovoltaic applications, where broad-spectrum solar absorption is essential for optimal device efficiency.

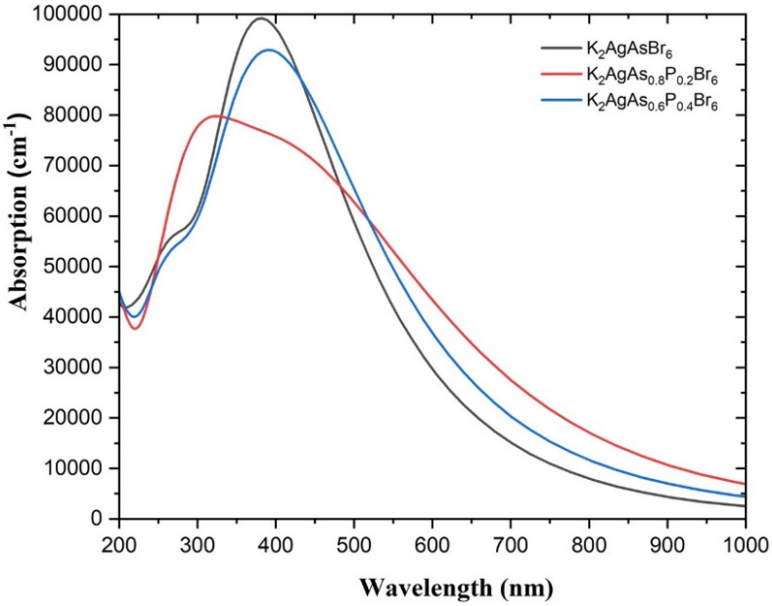

Figure 5. Absorption coefficients of $K_2AgAsBr_6$, $K_2AgAs_{0.8}P_{0.2}Br_6$, and $K_2AgAs_{0.6}P_{0.4}Br_6$.

3.2.2. Dielectric Function

The dielectric function, ε(ω), characterizes the material's response to electromagnetic radiation [19]. and can be expressed as:

$$\varepsilon(\omega) = \varepsilon_1(\omega) + i\varepsilon_2(\omega) \qquad (2)$$

The real part $\varepsilon_1(\omega)$ represents the polarization response, while the imaginary part $\varepsilon_2(\omega)$ describes energy absorption through electronic transitions [20]. Our calculations demonstrate that the static dielectric constant $\varepsilon_1(0)$ increases with P content, suggesting enhanced polarizability. The imaginary component exhibits a systematic red-shift of the main peak with increasing P content, consistent with the observed absorption spectra trends.

The dielectric function graphs presented in (Figure 6) illustrate the optical properties of $K_2AgAsBr_6$ and its P-doped variants ($K_2AgAs_{0.8}P_{0.2}Br_6$ and $K_2AgAs_{0.6}P_{0.4}Br_6$) across a wavelength range of 0-1000 nm [21]. The real part (Figure 6 a) exhibits characteristic oscillator behavior with an initial peak at approximately 200 nm, followed by a negative dip around 300-400 nm, and subsequently a steep rise beginning at 400 nm before plateauing at higher wavelengths, consistent with observations in related double perovskite Cs2AgBiBr6 [22]. The imaginary part (Figure 6 b) reveals distinct absorption peaks, with the pure $K_2AgAsBr_6$ displaying the sharpest peak near 500 nm. The incorporation of P-doping induces systematic shifts in peak positions and results in broader spectral features compared to the pure compound, analogous to effects observed in Cs2AgBiCl6 doped halide double perovskites [23]. This broadening and shifting of peaks with increased P content indicates significant modification of the material's electronic structure and optical properties. These spectral features are characteristic of semiconductor materials, where the peaks correspond to electronic transitions, and the overall shape reflects the material's response to electromagnetic radiation across different wavelengths.

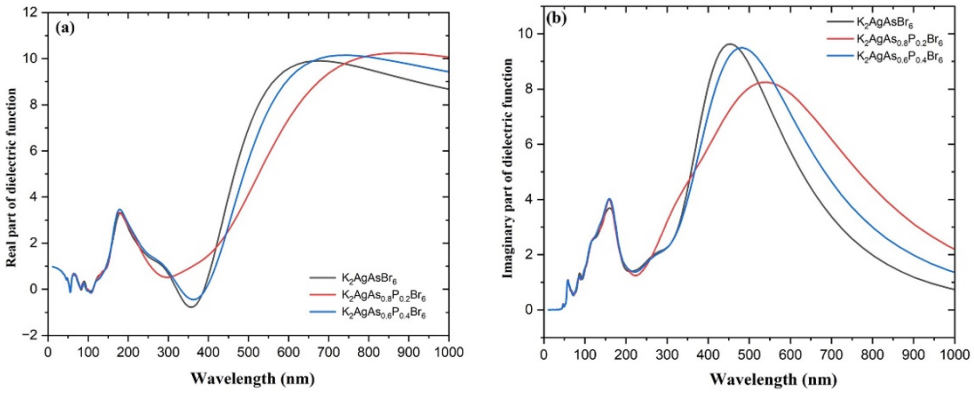

Figure 6. Real (a) and imaginary (b) parts of the dielectric function of $K_2AgAsBr_6$, $K_2AgAs_{0.8}P_{0.2}Br_6$, and $K_2AgAs_{0.6}P_{0.4}Br_6$.

3.2.3. Refractive Index

The refractive index, a key parameter quantifying how light propagates through a medium, was calculated for both pristine $K_2AgAsBr_6$ and its phosphorus-doped counterpart. The complex refractive index $n^*(\omega)$ is expressed as [24]:

$$n^*(\omega) = n(\omega) + ik(\omega) \quad (3)$$

where $n(\omega)$ is the refractive index and $k(\omega)$ is the extinction coefficient [25]. These components can be calculated using:

$$n(\omega) = 2\omega\sqrt{\frac{\varepsilon_1(\omega)}{2} + \sqrt{\frac{(\varepsilon_1(\omega))^2 + (\varepsilon_2(\omega))^2}{2}}} \quad (4)$$

$$k(\omega) = 2\omega\sqrt{\frac{-\varepsilon_1(\omega)}{2} + \sqrt{\frac{(\varepsilon_1(\omega))^2 + (\varepsilon_2(\omega))^2}{2}}} \quad (5)$$

Figure 7 display the optical properties of $K_2AgAsBr_6$ and its P-doped derivatives ($K_2AgAs_{0.8}P_{0.2}Br_6$ and $K_2AgAs_{0.6}P_{0.4}Br_6$) through their extinction coefficient (Figure 7 b) and refractive index (Figure 7 a) spectra across the 0-1000 nm wavelength range [26]. The refractive index patterns exhibit oscillating features at lower wavelengths (100-300 nm), followed by a sharp increase starting around 400 nm, ultimately reaching a plateau at higher wavelengths with values between 3.0-3.5, consistent with typical values observed in Cs2KBiCl6 double perovskite systems[27]. The extinction coefficient (Figure 7 b) reveals distinctive absorption peaks, with the undoped $K_2AgAsBr_6$ displaying the most pronounced peak at approximately 500 nm. The incorporation of phosphorus induces systematic changes in both optical parameters - the peaks broaden and shift positions, particularly in the visible region (400-700 nm), like effects observed in Cs2AgBiBr6 doped halide perovskites [28]. These spectral modifications indicate that P-doping significantly influences the material's electronic structure and optical response. The extended tail in the extinction coefficient at longer wavelengths for P-doped samples demonstrates modified absorption characteristics, which could be particularly relevant for optoelectronic applications. The correlation between these optical parameters provides valuable insights into the material's potential for various photonic and optoelectronic applications. The calculations reveal that both the refractive index and extinction coefficient exhibit systematic changes with P doping. The static refractive index increases with P content, suggesting a denser optical medium, while the extinction coefficient demonstrates a red-shift and peak broadening, confirming enhanced visible light absorption in P-substituted compounds.

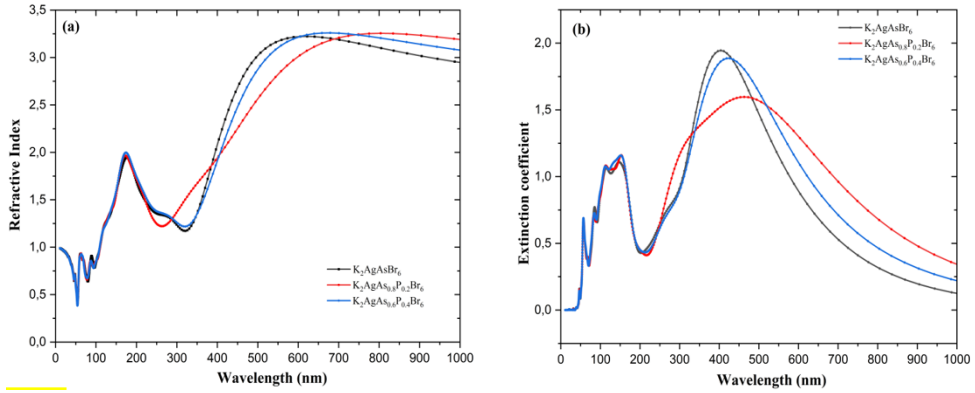

Figure 7. Refractive index (a) and extinction coefficient (b) of $K_2AgAsBr_6$, $K_2AgAs_{0.8}P_{0.2}Br_6$, and $K_2AgAs_{0.6}P_{0.4}Br_6$.

4. CONCLUSION

This comprehensive study provides compelling theoretical evidence for the effectiveness of phosphorus doping in tuning the optoelectronic properties of $K_2AgAsBr_6$ double perovskites. DFT calculations demonstrate that increasing phosphorus substitution systematically narrows the band gap through an upward shift of the valence band maximum, attributed to the higher energy of P 3p orbitals compared to As 4p orbitals. This finding is supported by the observed hybridization of P-p and As-p states at the valence band edge. The optical properties show consistent trends across all investigated parameters, with a characteristic red-shift and broadening of spectral features as P content increases. Notably, the P-substituted compounds demonstrate superior absorption in the visible light region, with $K_2AgAs_{0.6}P_{0.4}Br_6$ showing a remarkable 20% increase in absorption coefficient at 550 nm compared to the undoped compound, which could improve photovoltaic efficiency. These results suggest that phosphorus doping represents a promising strategy for enhancing the performance of $K_2AgAsBr_6$-based solar cells and optoelectronic devices. Future research directions should include experimental validation of these theoretical predictions, investigation of various synthesis techniques and doping concentrations, and exploration of alternative dopants such as halides or transition metals to further optimize the optoelectronic properties of $K_2AgAsBr_6$.

Author Contributions: A. Laassouli: Writing – original draft, Software, Investigation. L. Moulaoui: Writing – original draft, Software, Investigation. A. Najim: Writing – original draft, Software, Investigation. H. Errahoui: Writing – original draft, Software, Investigation. K. Rahmani: Supervision, Review & editing. Y. Lachtioui: Supervision, Review & editing. O. Bajjou: Supervision, Review & editing, Validation.

Funding: This article received no external funding.

Data Availability Statement: The data that supports the findings of this study are available from the corresponding author upon reasonable request.

Acknowledgments: The authors of this work would like to sincerely thank the Sultan Moulay Slimane University and UNISA university.

Conflicts of Interest: The authors have no affiliation with any organization with a direct or indirect financial interest in the subject matter discussed in the manuscript.

REFERENCES

[1] A. Kojima, K. Teshima, Y. Shirai, and T. Miyasaka, "Organometal Halide Perovskites as Visible-Light Sensitizers for Photovoltaic Cells," J Am Chem Soc, vol. 131, no. 17, pp. 6050–6051, May 2009,

doi: 10.1021/ja809598r.

[2] J. Barichello, G. Shankar, P. Mariani, A. Di Carlo, and F. Matteocci, "Unveiling the potential of Cs2AgBiBr6 perovskites for next-generation see-through photovoltaics," Mater Today Energy, vol. 46, p. 101725, Dec. 2024, doi: 10.1016/j.mtener.2024.101725.

[3] L. Moulaoui et al., "Numerical Simulation of FAPbI3 perovskite based solar cells with graphene oxide as hole transport layer using SCAPS-1D," in 2023 3rd International Conference on Innovative Research in Applied Science, Engineering and Technology (IRASET), IEEE, May 2023, pp. 1–7. doi: 10.1109/IRASET57153.2023.10153032.

[4] N. Al Aqtash et al., "First-principles calculations to investigate structural, mechanical, electronic, optical, and thermoelectric properties of novel cubic double Perovskites X2AgBiBr6 (X=Li, Na, K, Rb, Cs) for optoelectronic devices," Mol Simul, vol. 49, no. 16, pp. 1561–1572, Nov. 2023, doi: 10.1080/08927022.2023.2251604.

[5] H. Liu, J. Feng, and L. Dong, "Quick screening stable double perovskite oxides for photovoltaic applications by machine learning," Ceram Int, vol. 48, no. 13, pp. 18074–18082, Jul. 2022, doi: 10.1016/j.ceramint.2022.02.258.

[6] A. Laassouli, O. Bajjou, Y. Lachtioui, A. Najim, L. Moulaoui, and K. Rahmani, "DFT investigation on the electronic and optical properties of Br-doped CH3NH 3 SnI3 perovskite," in 2023 3rd International Conference on Innovative Research in Applied Science, Engineering and Technology (IRASET), IEEE, May 2023, pp. 1–6. doi: 10.1109/IRASET57153.2023.10153066.

[7] A. Ejjabli, M. Karouchi, M. Al-Hattab, O. Bajjou, K. Rahmani, and Y. Lachtioui, "Investigation of Lead-Free Halide K2AgSbBr6 Double Perovskite's Structural, Electronic, and Optical Properties Using DFT Functionals," Chemical Physics Impact, p. 100656, Jun. 2024, doi: 10.1016/j.chphi.2024.100656.

[8] H. Errahoui et al., "Impact of Calcium Doping on the Electronic and Optical Characteristics of Strontium Hydride (SrH2): A DFT Study," Atoms, vol. 12, no. 11, p. 55, Oct. 2024, doi: 10.3390/atoms12110055.

[9] A. Kumar, S. K. Tripathi, Mohd. Shkir, A. Alqahtani, and S. AlFaify, "Prospective and challenges for lead-free pure inorganic perovskite semiconductor materials in photovoltaic application: A comprehensive review," Applied Surface Science Advances, vol. 18, p. 100495, Dec. 2023, doi: 10.1016/j.apsadv.2023.100495.

[10] M. Karouchi et al., "Increasing Electro-Optical Properties of Perovskite FAPbI 3 Under the Effect of Doping by Sn," in 2023 3rd International Conference on Innovative Research in Applied Science, Engineering and Technology (IRASET), IEEE, May 2023, pp. 1–7. doi: 10.1109/IRASET57153.2023.10152963.

[11] A. Najim, O. Bajjou, A. Bakour, and K. Rahmani, "Electronic and optical properties of SWCNTs and spin-orbit coupling effect on their electronic structures: First-principle computing," J Electron Spectros Relat Phenomena, vol. 265, p. 147321, May 2023, doi: 10.1016/j.elspec.2023.147321.

[12] L. Moulaoui, O. Bajjou, A. Najim, and K. Rahmani, "The study of electronic and optical properties of perovskites CH 3 NH 3 PbCl 3 and CH 3 NH 3 PbBr 3 using first-principle," E3S Web of Conferences, vol. 336, p. 00015, Jan. 2022, doi: 10.1051/e3sconf/202233600015.

[13] L. Moulaoui et al., "Theoretical investigations on the electronic and optical properties of Na-doped CH 3 NH 3 PbI 3 perovskite," E3S Web of Conferences, vol. 469, p. 00086, Dec. 2023, doi: 10.1051/e3sconf/202346900086.

[14] A. Najim, O. Bajjou, A. Bakour, M. Boulghallat, and K. Rahmani, "A fundamental study on the electronic and optical properties of graphene oxide under an external electric field," Modern Physics Letters B, vol. 38, no. 10, Apr. 2024, doi: 10.1142/S0217984924500325.

[15] U. Saha, K. Debnath, and S. Satapathi, "Screening of potential double perovskite materials for photovoltaic applications using agglomerative hierarchical clustering," Nov. 2021.

[16] A. Najim, O. Bajjou, M. Boulghallat, K. Rahmani, and L. Moulaoui, "DFT study on electronic and optical properties of graphene under an external electric field," E3S Web of Conferences, vol. 336, p. 00006, Jan. 2022, doi: 10.1051/e3sconf/202233600006.

[17] Y. Zhang et al., "Photonics and optoelectronics using nano-structured hybrid perovskite media and their optical cavities," Phys Rep, vol. 795, pp. 1–51, Mar. 2019, doi: 10.1016/j.physrep.2019.01.005.

[18] X. Zhou, J. Jankowska, H. Dong, and O. V. Prezhdo, "Recent theoretical progress in the development of perovskite photovoltaic materials," Journal of Energy Chemistry, vol. 27, no. 3, pp. 637–649, May 2018, doi: 10.1016/j.jechem.2017.10.010.

[19] A. Najim et al., "Effects of lithium intercalation on the electronic and optical properties of graphene: Density Functional Theory (DFT) computing," in 2023 3rd International Conference on Innovative Research in Applied Science, Engineering and Technology (IRASET), IEEE, May 2023, pp. 1–5. doi: 10.1109/IRASET57153.2023.10153044.

[20] Md. A. Rahman et al., "First principles study on the structural, elastic, electronic, optical and thermal properties of lead-free perovskites CsCaX3(X=F, Cl, Br)," Physica B Condens Matter, vol. 669, p. 415260, Nov. 2023, doi: 10.1016/j.physb.2023.415260.

[21] M. R. Filip and F. Giustino, "Computational Screening of Homovalent Lead Substitution in Organic–Inorganic Halide Perovskites," The Journal of Physical Chemistry C, vol. 120, no. 1, pp. 166–173, Jan. 2016, doi: 10.1021/acs.jpcc.5b11845.

[22] C. N. Savory, A. Walsh, and D. O. Scanlon, "Can Pb-Free Halide Double Perovskites Support High-Efficiency Solar Cells?," ACS Energy Lett, vol. 1, no. 5, pp. 949–955, Nov. 2016, doi: 10.1021/acsenergylett.6b00471.

[23] B. Yang et al., "Lead-Free Direct Band Gap Double-Perovskite Nanocrystals with Bright Dual-Color Emission," J Am Chem Soc, vol. 140, no. 49, pp. 17001–17006, Dec. 2018, doi: 10.1021/jacs.8b07424.

[24] G. Nazir, A. Ahmad, M. F. Khan, and S. Tariq, "Putting DFT to the trial: First principles pressure dependent analysis on optical properties of cubic perovskite SrZrO3," Computational Condensed Matter, vol. 4, pp. 32–39, Sep. 2015, doi: 10.1016/j.cocom.2015.07.002.

[25] H. Lashgari, A. Boochani, A. Shekaari, S. Solaymani, E. Sartipi, and R. T. Mendi, "Electronic and optical properties of 2D graphene-like ZnS: DFT calculations," Appl Surf Sci, vol. 369, pp. 76–81, Apr. 2016, doi: 10.1016/j.apsusc.2016.02.042.

[26] M. Roknuzzaman et al., "Electronic and optical properties of lead-free hybrid double perovskites for photovoltaic and optoelectronic applications," Sci Rep, vol. 9, no. 1, p. 718, Jan. 2019, doi: 10.1038/s41598-018-37132-2.

[27] W. Meng, X. Wang, Z. Xiao, J. Wang, D. B. Mitzi, and Y. Yan, "Parity-Forbidden Transitions and Their Impact on the Optical Absorption Properties of Lead-Free Metal Halide Perovskites and Double Perovskites," J Phys Chem Lett, vol. 8, no. 13, pp. 2999–3007, Jul. 2017, doi: 10.1021/acs.jpclett.7b01042.

[28] A. H. Slavney, T. Hu, A. M. Lindenberg, and H. I. Karunadasa, "A Bismuth-Halide Double Perovskite with Long Carrier Recombination Lifetime for Photovoltaic Applications," J Am Chem Soc, vol. 138, no. 7, pp. 2138–2141, Feb. 2016, doi: 10.1021/jacs.5b13294.